Robust Co-optimization Planning of Interdependent Electricity and Natural Gas Systems with a Joint N-1 and Probabilistic Reliability Criterion

Chuan He Student Member, IEEE, Lei Wu Senior Member, IEEE, Tianqi Liu Senior Member, IEEE, Zhaohong Bie Senior Member, IEEE

Abstract— As the sharp growth of gas-fired power plants and the new emergence of Power-to-Gas (PtG) technology intensify the interdependency between electricity and natural gas systems, it is imperative to co-optimize the two systems for improving overall efficiency. This paper presents a long-term robust co-optimization planning model for interdependent systems, for minimizing total investment and operation costs. Beside generators, transmission lines, gas suppliers, and pipelines, PtGs and gas compressor stations are also considered as investment candidates to effectively handle wind power uncertainties in the power system and compensate pressure losses in the gas network. Furthermore, the proposed model includes a joint N-1 and probabilistic reliability criterion to promote economical and reliable planning solutions. The proposed model is solved via a decomposition approach, by iteratively solving a base-case master problem and two operation subproblems to check N-1 and probabilistic reliability criteria. Numerical case studies illustrate the effectiveness of the proposed robust co-optimization planning approach.

Index Terms— Co-optimization planning, power-to-gas, robust optimization, N-1 contingency, probabilistic reliability.

NOMENCLATURE

	-			
In	aı	0	00	٠,

d,l,b	Index of electrical loads/transmission lines/buses.
g,j,p,c,a	Index of gas loads/gas suppliers/pipelines/gas
	compressor stations/PtG facilities.
k,r	Index of identified worst cases/dual reliability cuts.
m,n	Indices of gas network nodes.

m,n Indices of gas network nodes.

Index of Monte Carlo (MC) sim

q Index of Monte Carlo (MC) simulation samples. t,h,i,w Index of years/load blocks/generators/wind farms.

Variables:

 AU_{iht} , AL_{lht} Binary variable which is equal to 1 if unit i/ line l is available, being 0 otherwise.

 ΔD_t^{bc} , ΔW_t^{bc} Base-case system load shedding/ wind spillage in year t.

 ΔD_t^{wc} Worst case system power imbalance in year t.

 f_{pht}^+ , f_{pht}^- Binary variables to indicate gas flow direction of pipeline p at load block h of year t.

 f_{cht}^+ , f_{cht}^- Operation status indicators of compressor station c at load block h of year t.

This work was supported in part by the U.S. National Science Foundation grants ECCS-1254310 and CMMI-1635339. C. He and T. Liu are with the School of Electrical Engineering and Information, Sichuan University, Chengdu, 610065, China (e-mail: jokerscu@stu.scu.edu.cn). L. Wu is with the ECE Department, Clarkson University, Potsdam, NY, 13699, USA (e-mail: lwu@clarkson.edu). Z. Bie is with the State Key Laboratory of Electrical Insulation and Power Equipment, Xi'an Jiaotong University, Xi'an, Shaanxi, 710049, China.

 G_{jht} , FC_{cht} Gas production of gas supplier j/ gas consumption of compressor station c at load block h of year t.

 G_{iht} , G_{aht} Gas consumption of gas-fired unit i/gas production of PtG facility a at load block h of year t.

IC,OC Investment/operation cost.

 P_{iht}^{bc} , P_{wht}^{bc} Dispatch of generator i/ wind farm w at load block h of year t in base case.

 P_{aht}^{bc} , v_{dht}^{bc} Base-case power consumption of PtG a/ load shedding of demand d at load block h of year t.

 PL_{lht}^{bc} , θ_{bht}^{bc} Base-case power flow of line l/ phase angle of electrical bus b at load block h of year t.

 Pr_{mht} Squared pressure of gas node m at load block h of year t

 Q_{pht} , Q_{cht} Gas flow in pipeline p/compressor station c at load block h of year t.

 s_{dht}^+ , s_{dht}^- Binary indicators for uncertainty set.

 y_{it} , y_{lt} , y_{at} Investment status of generator i/ transmission line l/PtG facility a in year t.

 z_{jt} , z_{pt} , z_{ct} Investment status of gas supplier j/ pipeline p/ compressor station c in year t.

 $(\cdot)^u$ Variables in response to uncertainties.

 $(\cdot)^{wc}$, $(\cdot)^{mc}$ Variables in worst case/MC simulation.

Constants:

 C^{I} , C^{W} Power imbalance/ wind spillage cost.

C^{re} Threshold of wind power recourse cost.

 C^{inv} Investment cost of a new electricity/gas asset.

 C_i^{fuel} , T_i^{retire} Fuel price/retirement year of unit i.

 C_j^{pro} Production cost of gas supplier j.

DT,dr Time duration and discount rate.

 D_{dht}^{bc} , G_{ght} Forecast value of electrical load d/gas load g at load block h of year t.

 \tilde{D}_{dht} , \tilde{P}_{wht} Load/wind deviation from forecast value of load d/wind farm w at load block h of year t.

 e_c^{com} , e_a^{ptg} Efficiency of compressor station c/PtG facility a.

Coefficient of present-worth value. K_{mn} Gas flow constant of pipeline mn.

M A large enough positive number.

ND,NW Number of electrical loads/wind farms. *NT,NH,NS* Number of years/load blocks/ MC samples.

 $P_{f,wht}^{bc}$ Wind power forecast of wind farm w at load block

h of year t.

 Pr_m^l, Pr_m^u Squared pressure lower/upper bound of node m.

 R_{ht} System spinning reserve at load block h of year t.

 R_i^{up} , R_i^{down} Up/down ramping limit of unit *i*.

s(l), r(l) Sending/receiving bus of transmission line l.

 X_l Reactance of transmission line l.

 y_{it}^{retire} Retirement status of unit *i* in year *t*.

 Δ_{dt} , Δ_{wt} Budget of electrical load/wind uncertainty in year t.

 Γ_c Compressor factor.

 $(\cdot)^{\min/\max}$ Min/max value of a quantity.

Functions and Sets:

CG,CL,CA Set of candidate units/transmission lines/PtGs.

CS,CP,CC Set of candidate gas suppliers/pipelines/compressor stations.

D,**W** Uncertainty set of electrical load/wind generation.

EG,EL,EA Set of existing units/transmission lines/PtGs.

ES,EP,EC Set of existing gas suppliers/pipelines/compressor stations.

 $F_i(\cdot)$ Heat rate curve of generator i.

GU Set of gas-fired generators

 $L^{g}(\cdot), L^{pg}(\cdot)$ Compact forms of certain system constraints.

N(b), G(m) Set of components at electric bus b/g as node m.

I. INTRODUCTION

Owing to distinct advantages of gas-fired generators over traditional fossil units, including lower capital cost, higher efficiency, faster response capability, and lower carbon emission, gas consumption by the power system has shown a sharp growth from 27% in 2005 to 39% in 2016 [1]. In addition, a new promising technology, Power-to-Gas (PtG), is being deployed to effectively convert excessive electric energy, especially from wind, into compatible gas [2]-[3].

Indeed, the growing reliance of the electricity grid on the natural gas network has significantly intensified interaction of the two systems, and brings new challenges on the reliability and efficiency of both systems. Specifically, different from fossil units whose fuel supply has been traditionally considered sufficient, gas-fired units rely on just-in-time gas supply from the natural gas network. In addition, PtG facilities count on the natural gas network to absorb gas converted from excessive wind energy. Consequently, co-optimization planning is in urgent need for strengthening the reliability and sustainability interdependent energy infrastructures. In co-optimization planning models have been actively sought by regional energy market operators [4]-[5] and federal agents [6].

The co-optimization planning problem of interdependent electricity and gas systems determines the type, capacity, location, and time of new components to be invested over the planning horizon, in order to ensure reliable and cost-effective power/gas production and delivery to meet electricity/gas demands. Such components in interdependent energy infrastructures would include generators, transmission lines, PtG facilities, gas suppliers, pipelines, and compressor stations.

Some literatures have studied expansion planning of integrated energy systems [7]-[13]. A long-term, multiarea, and multistage model for the expansion planning of integrated electricity and gas system is studied in [7], while considering the whole natural gas value chain. Reference [8] develops a combined gas and electricity network expansion planning model to invest in new pipelines, compressors, storages facilities, and transmission lines. Market interactions among various stakeholders are considered in [9], which models alternating current (AC) power flow of the power system and nonlinear nature of the gas network. A transportation model of the gas network is incorporated in the co-planning model in [10], which is solved by an interactive process between a least-cost investment master problem and two operation subproblems representing physical feasibility and financial optimality. The authors in [11]-[12] further consider power system uncertainties such as demand growth, energy price, and government policies in the co-planning model for a combined electricity and gas market. An integrated multi-period three-stage model is studied in [13] to determine optimal generation, transmission, and natural gas network expansions.

Reliable electricity delivery is of the core value in the entire power industry, and the N-1 criterion is widely used in power system planning as a deterministic approach to ensure reliability [14]-[15]. The N-1 standard requires that the normal operation should be maintained, i.e., without any loss-of-load, under any single contingency outage. However, the deterministic N-1 standard neglects the stochastic nature of simultaneous outage of multiple generators and transmission lines. Alternatively, probabilistic models consider reliability criteria, such as loss-of-load-expectation (LOLE), loss-ofenergy-probability (LOEP) and expected-energy-not -supplied (EENS), in expansion planning of power systems [16]-[18]. Indeed, it is mentioned in [19] that the N-1 criterion may lead to over-investment solutions, while probabilistic approaches, focusing on high-probability/low- damage events to derive low investment costs, could leave the system vulnerable to low-probability/high-damage events. Both deterministic N-1 and probabilistic reliability criteria are adopted in [20] to evaluate reliable planning of power systems.

This paper proposes an adjustable robust optimization based co-optimization planning model for interdependent electricity and natural gas systems, which minimizes the total investment and operation costs of the two systems while considering power system uncertainties. Specifically, due to variability and uncertainty of wind power, wind spillage has long been an issue [21]-[22]. This paper focuses on investing in new gas-fired units and PtG facilities in the planning stage, and adopting wind power recourse cost to mitigate wind spillage under uncertainties. In addition, both N-1 and probabilistic reliability criteria are incorporated into the co-optimization framework, so that low-probability/high-impact events are adequately addressed while overall reliability is also ensured. Unlike the power system, the gas network is regarded highly reliable and the N-1 criterion does not apply [11]-[12]. Thus, uncertainty and curtailment of non-generation gas loads are not considered.

Major contributions of the paper are threefold.

(1.3)

- 1) Modeling of Interdependent Systems: Compared with [7]-[13] which consider generators, transmission lines, gas suppliers, and pipelines in expansion planning of integrated energy systems, the proposed co-optimization planning model also considers PtGs and gas compressor stations as investment candidates for facilitating a deeper penetration of wind energy and compensating gas pressure losses with a proliferation of gas-fired units. Moreover, retirement of traditional coal-fired units is also considered. In addition, as compressor stations typically consume about 3-5% of the total transported gas [23], gas consumption of compressor stations is rigorously modeled, which has been neglected in [7], [10]-[11], [13].
- 2) Wind Power Utilization: To further avoid extensive wind spillage under uncertainties and promote PtG facilities, wind power recourse cost is proposed within the robust optimization framework for enhancing wind power utilization. Similar to the recourse cost for restricting re-dispatch cost in [24], wind power recourse cost proposed in this paper can effectively limit wind spillage quantities when various uncertainties are revealed.
- 3) Reliability Evaluation Criterion: Compared with methods in [14]-[15] which only consider the N-1 criterion and methods in [16]-[19] which only explore the probabilistic reliability criterion for power system planning, this paper extends the robust optimization model to include a joint N-1 and probabilistic reliability criterion for further promoting reliable and economical co-optimization planning solutions. low-probability/high-impact That is, damages corresponding to worst case realizations of uncertain electrical loads, wind generations, and contingencies are mitigated by the max-min N-1 subproblem, while the overall system reliability with respect to random outages of generators and transmission lines is guaranteed by the probabilistic reliability subproblem. Reference [20] discusses a joint deterministic-probabilistic criterion to evaluate reliability performance for a set of predefined planning strategies. In comparison, this paper investigates optimal planning solutions by integrating the N-1 criterion and probabilistic reliability criterion into a robust optimization framework.

The rest of the paper is organized as follows. Sections II-III discuss the proposed robust co-optimization planning model and the solution methodology. Numerical case studies are presented in Section IV, and Section V concludes the paper.

II. MODEL DESCRIPTION

This section presents the mathematical formulation of the proposed robust co-optimization planning model, which considers uncertainties in electrical loads/wind generations, N-1 contingencies, and the overall system reliability. Although a finer temporal model such as time-series could better capture the stochastic nature and temporal correlation of renewable energy, it may be computationally intractable in the long-term planning problem due to the curse of dimensionality. Furthermore, the LOLE index, as a long-term reliability criterion used in power system planning, is traditionally calculated using daily peak loads or load blocks [16], [25]-[27].

In turn, following the convention of optimization-based power system planning [10], [15], [28], this paper adopts several blocks to represent typical correlated load levels and renewable energy outputs in multiple hours of each planning year.

A. Objective Function

The proposed robust co-optimization planning model of electricity and natural gas systems is to minimize the total costs associated with electricity/gas asset investments, electricity/gas system operation, electrical load imbalance, and wind spillage (1.1). Equation (1.2) calculates investment costs of generators, transmission lines, PtGs, gas suppliers, gas pipelines, and compressor stations. Equation (1.3) represents operation costs of electricity and gas systems, in which operation costs of gas-fired units are considered in terms of gas fuel cost and carried out by gas production costs. Coefficient of presentworth value is calculated as $\kappa_t = 1/(1+dr)^{t-1}$.

The proposed model is from the viewpoint of a cooperator of power and gas systems, while the objective (1.3) includes the total production costs of the power system and the gas network. The production cost of the gas network is represented as $\sum \sum \sum \kappa_t \cdot DT_{ht} \cdot C_j^{\text{pro}} \cdot G_{jht}$, while the production cost of the

power system potentially includes costs of non-gas thermal units
$$\sum_{t} \sum_{h} \sum_{i \notin GU} \kappa_t \cdot DT_{ht} \cdot C_i^{\text{fuel}} \cdot F_i \left(P_{iht}^{bc} \right)$$
 and gas units.

However, as gas-fired units consume natural gas and are regarded as gas loads in the gas network, different from non-gas thermal units, their costs are indirectly calculated via the production cost of natural gas suppliers.

$$\min \left(IC + OC + C^{I} \cdot \sum_{t} \Delta D_{t}^{bc} + C^{W} \cdot \sum_{t} \Delta W_{t}^{bc} \right)$$

$$IC = \sum_{t} \sum_{i \in CG} \kappa_{t} \cdot C_{i}^{inv} \cdot y_{it} + \sum_{t} \sum_{l \in CL} \kappa_{t} \cdot C_{l}^{inv} \cdot y_{lt}$$

$$+ \sum_{t} \sum_{a \in CA} \kappa_{t} \cdot C_{a}^{inv} \cdot y_{at} + \sum_{t} \sum_{j \in CS} \kappa_{t} \cdot C_{j}^{inv} \cdot z_{jt}$$

$$+ \sum_{t} \sum_{p \in CP} \kappa_{t} \cdot C_{p}^{inv} \cdot z_{pt} + \sum_{t} \sum_{c \in CC} \kappa_{t} \cdot C_{c}^{inv} \cdot z_{ct}$$

$$OC = \sum_{t} \sum_{h} \sum_{i \notin GU} \kappa_{t} \cdot DT_{ht} \cdot C_{i}^{fuel} \cdot F_{i} \left(P_{iht}^{bc} \right)$$

$$(1.1)$$

B. Investment Constraints

 $+ \sum_{t} \sum_{h} \sum_{j} \kappa_{t} \cdot DT_{ht} \cdot C_{j}^{\text{pro}} \cdot G_{jht}$

The co-optimization planning model considers investments in units, transmission lines, PtGs, gas suppliers, pipelines, and compressor stations. Once a candidate is installed, its investment status will be fixed to 1 for the remaining years (2.1)-(2.6). Retirement of existing units within the planning horizon is also considered. That is, operation status of an existing unit is switched to 0 after retirement (2.7). Constraint (2.8) ensures that the total generation capacity can meet forecasted electrical loads plus system reserve. Constraint (3) describes the annual LOLE criterion, which is a widely

accepted probabilistic method for evaluating power system reliability. However, explicit analytical formula for (3) is not readily available, as annual system LOLE is a probabilistic criterion which depends on investment decisions as well as electrical loads and available wind energy. In this paper, (3) will be rigorously evaluated in the probabilistic reliability checking subproblem as discussed in Section III.C.

$$y_{i(t-1)} \le y_{it}, \qquad i \in \mathbf{CG} \tag{2.1}$$

$$y_{l(t-1)} \le y_{lt}, \qquad l \in CL \tag{2.2}$$

$$y_{a(t-1)} \le y_{at}, \qquad a \in CA \tag{2.3}$$

$$z_{i(t-1)} \le z_{it}, \qquad j \in \mathbf{CS} \tag{2.4}$$

$$z_{p(t-1)} \le z_{pt}, \qquad p \in \mathbf{CP} \tag{2.5}$$

$$z_{c(t-1)} \le z_{ct}, \qquad c \in \mathbf{CC} \tag{2.6}$$

$$y_{it}^{\text{retire}} = 0, t \ge T_i^{\text{retire}}, \qquad i \in \mathbf{EG}$$
 (2.7)

$$\sum_{i \in EG} P_i^{\text{max}} \cdot y_{it}^{\text{retire}} + \sum_{i \in CG} P_i^{\text{max}} \cdot y_{it} \ge \sum_{d} D_{dht}^{bc} + R_{ht}$$
 (2.8)

$$LOLE\left(y_{it}, y_{lt}, D_{dht}^{bc}, P_{f, wht}^{bc}\right) \le LOLE^{\max}$$
 (3)

C. Operation Constraints

The proposed planning model also evaluates operation constraints for the power system and the gas network, as well as their operational interdependency. Power system operation constraints (4) describe operating conditions of units, transmission lines, buses, wind farms, and PtGs in the base case. Equation (4.1) represents nodal power balance. Constraint (4.2)-(4.3) limits annual system load shedding in the base case. Annual system wind spillage in base case is calculated in (4.4). Using DC power flow model, constraints (4.5)-(4.8) enforce power flow limits of existing and candidate lines. Bus phase angles are limited by (4.9). Constraints (4.10)-(4.14) enforce capacity limits of existing/ candidate generators, existing/ candidate PtGs and wind farms. Equation (4.14) represents that wind power is dispatchable in the way of wind curtailment. That is, wind generation is modeled as a dispatchable resource because wind power can be spilled to maintain the operation security of power systems, especially in high wind and low load situations [28]-[29].

$$\sum_{i \in N(b)} P_{iht}^{bc} + \sum_{w \in N(b)} P_{wht}^{bc} - \sum_{s(l) \in N(b)} PL_{lht}^{bc} + \sum_{r(l) \in N(b)} PL_{lht}^{bc}
- \sum_{a \in N(b)} P_{aht}^{bc} + \sum_{d \in N(b)} v_{dht}^{bc} = \sum_{d \in N(b)} D_{dht}^{bc}$$
(4.1)

$$\Delta D_t^{bc} = \sum_{b} \sum_{d} DT_{ht} \cdot v_{dht}^{bc}$$
 (4.2)

$$\Delta D_t^{bc} \le \Delta D_t^{bc, \text{max}} \tag{4.3}$$

$$\Delta W_t^{bc} = \sum_{h} \sum_{w} DT_{ht} \cdot \left(P_{f,wht}^{bc} - P_{wht}^{bc} \right)$$

$$\tag{4.4}$$

$$PL_{lht}^{bc} \cdot X_l = \left(\theta_{s(l)ht}^{bc} - \theta_{r(l)ht}^{bc}\right), \qquad l \in EL$$
 (4.5)

$$-PL_{l}^{\max} \le PL_{lht}^{bc} \le PL_{l}^{\max}, \qquad l \in \mathbf{EL}$$
 (4.6)

$$-PL_{l}^{\max} \cdot y_{lt} \le PL_{lht}^{bc} \le PL_{l}^{\max} \cdot y_{lt}, \qquad l \in CL$$
 (4.7)

$$- \left(1 - y_{lt}\right) \cdot M \leq PL_{lht}^{bc} \cdot X_l - \left(\theta_{s(l)ht}^{bc} - \theta_{r(l)ht}^{bc}\right) \leq \left(1 - y_{lt}\right) \cdot M,$$

$$l \in CL$$
 (4.8)

$$-\theta_h^{\text{max}} \le \theta_{hht}^{bc} \le \theta_h^{\text{max}} \tag{4.9}$$

$$0 \le P_{iht}^{bc} \le P_i^{\text{max}} \cdot y_{it}^{\text{retire}}, \qquad i \in \mathbf{EG}$$
 (4.10)

$$0 \le P_{iht}^{bc} \le P_i^{\max} \cdot y_{it}, \qquad i \in \mathbf{CG}$$
 (4.11)

$$0 \le P_{aht}^{bc} \le P_a^{\text{max}}, \qquad a \in \mathbf{E}\mathbf{A}$$
 (4.12)

$$0 \le P_{aht}^{bc} \le P_a^{\text{max}} \cdot y_{at}, \qquad a \in \mathbf{CA}$$
 (4.13)

$$0 \le P_{wht}^{bc} \le P_{f,wht}^{bc} \tag{4.14}$$

Gas network model (5) describes operating characteristics of the gas system via Weymouth gas flow equations [30]. Gas network nodal balance equation (5.1) describes that the total gas flow injection is equal to the total withdrawn at each node. Production limits of existing and candidate gas suppliers are shown in (5.2)-(5.3). Constraint (5.4) represents the pressure limit of each gas node. Nonlinear Weymouth equations (5.5)-(5.6) describe the relationship between squared nodal pressure and pipeline flow rates. Gas flow directions of pipelines are determined by (5.7)-(5.9), where $f_{pht}^+ = 1/f_{pht}^+$

 $f_{pht}^-=1$ indicates that gas flows from node m/n to node n/m through pipeline p. Constraints (5.10)-(5.20) describe operating characteristics of compressor stations. Equations (5.10)-(5.12) calculate terminal gas pressures of existing and candidate compressor stations [31] with node m/n as primary/secondary side. Constraints (5.13)-(5.15) describe operation status of a compressor station, where $f_{cht}^+=1/f_{cht}^-=1$ indicates that a compressor station is not/is operating. Constraints (5.16)-(5.20) describe gas fuel consumptions of existing and candidate compressor stations [23], which consume gas only if they are invested and in operation.

$$\sum_{j \in G(m)} G_{jht} - \sum_{s(p) \in G(m)} Q_{pht} + \sum_{r(p) \in G(m)} Q_{pht} - \sum_{s(c) \in G(m)} Q_{cht} + \sum_{r(c) \in G(m)} \left(Q_{cht} - FC_{cht}\right) + \sum_{a \in G(m)} G_{aht} - \sum_{i \in G(m)} G_{iht} = \sum_{g \in G(m)} G_{ght}$$

$$(5.1)$$

$$0 \le G_{iht} \le G_i^{\text{max}}, \qquad j \in \mathbf{ES} \qquad (5.2)$$

$$0 \le G_{jht} \le G_j^{\text{max}} \cdot z_{jt}, \qquad j \in \mathbf{CS} \qquad (5.3)$$

$$Pr_m^{\min} \le Pr_{mht} \le Pr_m^{\max} \tag{5.4}$$

$$\left(f_{pht}^{+} - f_{pht}^{-}\right) \cdot \left(Pr_{mht} - Pr_{nht}\right) = Q_{pht}^{2} / K_{mn}^{2}, p \in \mathbf{EP}$$
 (5.5)

$$z_{pt} \cdot \left(f_{pht}^+ - f_{pht}^-\right) \cdot \left(Pr_{mht} - Pr_{nht}\right) = Q_{pht}^2 / K_{mn}^2, p \in \mathbf{CP} \tag{5.6}$$

$$-\left(1 - f_{pht}^{+}\right) \cdot M \le Q_{pht} \le \left(1 - f_{pht}^{-}\right) \cdot M, \qquad p \in \mathbf{EP} \cup \mathbf{CP} \tag{5.7}$$

$$f_{pht}^{+} + f_{pht}^{-} = 1,$$
 $p \in EP \cup CP$ (5.8)

$$-\left(1-f_{pht}^{+}\right)\cdot M \leq Pr_{mht} - Pr_{nht} \leq \left(1-f_{pht}^{-}\right)\cdot M$$

 $p \in \mathbf{EP} \cup \mathbf{CP}$ (5.9)

$$\Gamma_c^2 \cdot Pr_{mht} \ge Pr_{nht}, \qquad c \in EC$$
 (5.10)

$$-z_{ct} \cdot M \le Pr_{nht} - Pr_{mht} \le z_{ct} \cdot M, \qquad c \in CC$$
 (5.11)

$$Pr_{nht} - \Gamma_c^2 \cdot Pr_{mht} \le (1 - z_t) \cdot M, \qquad c \in \mathbb{CC}$$
 (5.12)

$$-\left(1-f_{cht}^{+}\right)\cdot M \leq Pr_{mht} - Pr_{nht} \leq \left(1-f_{cht}^{+}\right)\cdot M,$$

$$c \in EC \cup CC \quad (5.13)$$

$$Pr_{mht} - Pr_{nht} \leq \left(1-f_{cht}^{-}\right)\cdot M, \qquad c \in EC \cup CC \quad (5.14)$$

$$f_{cht}^{+} + f_{cht}^{-} = 1, \qquad c \in EC \cup CC \quad (5.15)$$

$$-\left(1-f_{cht}^{+}\right)\cdot M \leq FC_{cht} \leq \left(1-f_{cht}^{+}\right)\cdot M, \quad c \in EC \quad (5.16)$$

$$-\left(1-f_{cht}^{-}\right)\cdot M \leq FC_{cht} - \left(1-e_{c}^{com}\right)\cdot Q_{cht} \leq \left(1-f_{cht}^{-}\right)\cdot M,$$

$$c \in EC \quad (5.17)$$

$$0 \leq FC_{cht} \leq z_{ct} \cdot M, \qquad c \in CC \quad (5.18)$$

$$-\left(2-z_{ct}-f_{cht}^{+}\right)\cdot M \leq FC_{cht} \leq \left(2-z_{ct}-f_{cht}^{+}\right)\cdot M,$$

$$c \in CC \quad (5.19)$$

$$-\left(2-z_{ct}-f_{cht}^{-}\right)\cdot M \leq FC_{cht} - \left(1-e_{c}^{com}\right)\cdot Q_{cht} \quad (5.20)$$

$$\leq \left(2-z_{ct}-f_{cht}^{-}\right)\cdot M, c \in CC$$

Electricity and gas systems are linked by gas-fired units and PtGs, which are regarded as generators/gas loads and electrical loads/gas suppliers in electricity/gas system. Constraint (6.1) describes the relationship between power dispatch and gas consumption of gas-fired units via heat rate curve and high heating value (HHV). PtGs are modeled via energy conversion factor ϕ , efficiency e_a^{ptg} , and HHV as in (6.2), where HHV= 1.026MBtu/kcf and ϕ =3.4MBtu/MWh. For the sake of discussion, gas network constraints (5) and coupling constraints (6) are rewritten in a compact form as in (7).

$$G_{iht} = F_i \left(P_{iht}^{bc} \right) / \text{HHV}, \qquad i \in \mathbf{GU}$$
 (6.1)

$$G_{aht} = \phi \cdot P_{aht}^{bc} \cdot e_a^{\text{ptg}} / \text{HHV}$$
 (6.2)

$$\boldsymbol{L}^{g}\left(P_{iht}^{bc}, P_{aht}^{bc}\right) \le 0 \tag{7}$$

Constraints (8)-(9) evaluate operation security, in terms of maximum annual power imbalance in the worst case, of interdependent systems in response to uncertainties of electrical load, wind generation, and N-1 contingencies. That is, the annual largest possible load imbalance under uncertainties is identified via (8), which is further limited by the annual power imbalance threshold as in (9). Constraint (8.2) describes the N-1 criterion, i.e., at most one generator/ transmission line is on contingency outage. Constraints (8.3)-(8.5) describe load and wind uncertainty sets. Take load uncertainty set D as an example. If $s_{dht}^+ = 1/s_{dht}^- = 1$, uncertain electrical load d reaches its upper/lower limit at load block h of year t; if both are 0, the forecasted load value is achieved. In addition, budget constraints in (8.3)-(8.4) control total deviations of loads and wind generations from their forecast values, where budgets of uncertainty Δ_{dt} and Δ_{wt} take values between 0 and NH. Note that in uncertainty sets (8.3)-(8.4), D_{dht}^{bc} and $P_{f,wht}^{bc}$ are base case forecasted values of electrical loads and wind powers in each year, which have already reflected average annual growths of peak electrical load and wind power, while deviations \tilde{D}_{dht}

and \tilde{P}_{wht} from the base values are used to simulate the combined effect of short-term variability and long-term annual growth uncertainty.

Constraints (8.6)-(8.20) describe operation characters of interdependent systems in response to uncertainty realizations of electrical load D_{dht}^u , wind $P_{f,wht}^u$, and contingencies AU_{iht} / AL_{lht} . Specifically, dispatch adjustments of generators/wind farms/PtGs $P_{iht}^u / P_{wht}^u / P_{aht}^u$ in response to uncertainties need to satisfy system load balance (8.6), power flow equations (8.7)-(8.8), power flow limits (8.9)-(8.10), bus phase angle limits (8.11), and capacity limits (8.12)-(8.16). Dispatches in the base case and under uncertainties are further coupled via ramping capabilities (8.17). Wind power is traditionally modeled as a dispatchable resource in robust optimization, as wind power can be spilled for maintaining the security of power systems [28]-[29]. In this paper, in order to effectively utilize available wind energy in the worst case and promote more PtGs, the wind power recourse cost is adopted to limit wind spillage quantities under uncertainties (8.18), i.e., the annual wind spillage penalty cannot exceed the budget. Constraint (8.19) ensures non-negativity of power mismatch variables. Natural gas network feasibility under uncertainties is guaranteed by (8.20). In (8), symbols bracketed in the end are dual variables of corresponding constraints. For the sake of discussion, operation constraints under uncertainties (8.6)-(8.20) and (9) are further presented in a compact form as in

$$\Delta D_t^{wc} = \max \min \sum_{h} \sum_{d} DT_{ht} \cdot \left(v_{dht}^{+u} + v_{dht}^{-u} \right)$$
 (8.1)

s.t.
$$\sum_{i} (1 - AU_{iht}) + \sum_{l} (1 - AL_{lht}) \le 1$$
 (8.2)

$$\mathbf{D} = \begin{cases} D_{dht}^{u} \in \mathbb{R}^{ND \times NH \times NT} : \sum_{h} s_{dht}^{+} + s_{dht}^{-} \le \Delta_{dt}, s_{dht}^{+} + s_{dht}^{-} \le 1 \\ D_{dht}^{u} = D_{dht}^{bc} + s_{dht}^{+} \cdot \tilde{D}_{dht} - s_{dht}^{-} \cdot \tilde{D}_{dht}, s_{dht}^{+}, s_{dht}^{-} \in \{0, 1\} \end{cases}$$
(8.3)

$$\mathbf{W} = \begin{cases} P_{f,wht}^{u} \in \mathbb{R}^{NW \times NH \times NT} : \sum_{h} s_{wht}^{+} + s_{wht}^{-} \leq \Delta_{wt}, s_{wht}^{+} + s_{wht}^{-} \leq 1 \\ P_{f,wht}^{u} = P_{f,wht}^{bc} + s_{wht}^{+} \cdot \tilde{P}_{wht} - s_{wht}^{-} \cdot \tilde{P}_{wht}, s_{wht}^{+}, s_{wht}^{-} \in \{0,1\} \end{cases}$$

 $D_{dht}^{u} \in \mathbf{D}, P_{f \ wht}^{u} \in \mathbf{W} \tag{8.5}$

$$\sum_{i \in N(b)} P_{lht}^{u} + \sum_{w \in N(b)} P_{wht}^{u} - \sum_{s(l) \in N(b)} PL_{lht}^{u} + \sum_{r(l) \in N(b)} PL_{lht}^{u}$$

$$- \sum_{a \in N(b)} P_{aht}^{u} + \sum_{d \in N(b)} \left(v_{dht}^{+u} - v_{dht}^{-u} \right) = \sum_{d \in N(b)} D_{dht}^{u} : (\beta_{bht})$$
(8.6)

$$PL_{lht}^{u} \cdot X_{l} = AL_{lht} \cdot \left(\theta_{s(l)ht}^{u} - \theta_{r(l)ht}^{u}\right), \quad l \in EL : \left(\chi_{lht}\right)$$
 (8.7)

$$-(1 - y_{lt} \cdot AL_{lht}) \cdot M \le PL_{lht}^{u} \cdot X_{l} - (\theta_{s(l)ht}^{u} - \theta_{r(l)ht}^{u})$$

$$\le (1 - y_{lt} \cdot AL_{lht}) \cdot M, l \in CL : (\eta_{lht}, \gamma_{lht})$$
(8.8)

$$-PL_{l}^{\max} \leq PL_{lht}^{u} \leq PL_{l}^{\max}, \qquad l \in \mathbf{EL}: (\mu_{lht}, \lambda_{lht})$$
(8.9)

$$-PL_{l}^{\max} \cdot y_{lt} \cdot AL_{lht} \leq PL_{lht}^{u} \leq PL_{l}^{\max} \cdot y_{lt} \cdot AL_{lht},$$

$$l \in CL : (\delta_{lht}, \pi_{lht})$$
(8.10)

$$-\theta_b^{\max} \le \theta_{bht}^u \le \theta_b^{\max} : (\varepsilon_{bht}, \alpha_{bht})$$
(8.11)

$$0 \le P_{iht}^{u} \le P_{i}^{\text{max}} \cdot y_{it}^{\text{retire}}, \qquad i \in \mathbf{\textit{EG}} : (\sigma_{iht})$$
 (8.12)

$$0 \le P_{iht}^{u} \le P_{i}^{\max} \cdot y_{it}, \qquad i \in \mathbf{CG} : (\xi_{iht})$$
 (8.13)

$$0 \le P_{aht}^{u} \le P_{a}^{\max}, \qquad a \in \mathbf{EA} : (\zeta_{aht})$$
 (8.14)

$$0 \le P_{aht}^{u} \le P_{a}^{\max} \cdot y_{at}, \qquad a \in \mathbf{CA} : (v_{aht})$$
 (8.15)

$$0 \le P_{wht}^u \le P_{f,wht}^u : (\rho_{wht}) \tag{8.16}$$

$$\left(P_{iht}^{bc} - R_i^{\text{down}}\right) \cdot AU_{iht} \le P_{iht}^{u} \le \left(P_{iht}^{bc} + R_i^{\text{up}}\right) \cdot AU_{iht} : \left(\varphi_{iht}, \psi_{iht}\right)$$
(8.17)

$$\sum_{h} \sum_{w} C^{W} \cdot DT_{ht} \cdot \left(P_{f, wht}^{u} - P_{wht}^{u} \right) \le C_{t}^{\text{re}} : \left(\Omega_{t} \right)$$
(8.18)

$$v_{dht}^{+u} \ge 0, v_{dht}^{-u} \ge 0$$
 (8.19)

$$\boldsymbol{L}^{g}\left(P_{iht}^{u}, P_{aht}^{u}\right) \le 0 \tag{8.20}$$

$$\Delta D_t^{wc} \le \Delta D_t^{wc, \text{max}} \tag{9}$$

$$\boldsymbol{L}^{\text{pg}}\left(P_{iht}^{u}, P_{wht}^{u}, P_{aht}^{u}, D_{dht}^{u}, P_{f,wht}^{u}, AL_{lht}, AU_{iht}, v_{dht}^{+u}, v_{dht}^{-u}\right) \leq 0$$
(10)

III. SOLUTION METHODOLOGY

The proposed robust planning problem (1)-(6) and (8)-(9) includes three optimization levels: (i) the upper level (1)-(6) which determines optimal investment and operation decisions of electricity and natural gas systems in the base case. In addition, the probabilistic reliability constraint (3) ensures that the investment of assets can meet the overall system reliability requirement; (ii) the middle level (8.2)-(8.5) which identifies worst-case scenarios with the highest load imbalance corresponding to the solution from the upper level, with respect to N-1 contingencies and uncertainties of electrical loads and wind generations; and (iii) the lower level (8.6)-(8.20) which determines dispatches of electricity and natural gas systems for minimizing the system load imbalance, given upper level investment decisions and middle level uncertainty realizations.

The proposed robust co-optimization planning model may not be effectively solved without decomposition, especially in recognizing the challenges from probabilistic reliability constraint (3) and max-min security evaluation (8). A decomposition based approach is adopted to effectively solve the problem, by iteratively optimizing base-case investment/ operation decisions in a master problem and checking solution quality of the master problem via N-1 and probabilistic reliability criteria in two subproblems. The N-1 security checking max-min subproblem generates primal cuts (via the column-and-constraint generation approach [24], [32]) and the probabilistic reliability subproblem generates dual cuts (via the Benders decomposition method [10], [17]). Note that the N-1 security checking subproblem and the probabilistic reliability subproblem are carried out for each year.

A. Master Problem

The master problem is presented as in (11), in which worst

case realizations D^{wc}_{dht} , $P^{wc}_{f,wht}$, AU^{wc}_{iht} and AL^{wc}_{lht} identified in the N-1 security subproblem in Section III.B and dual reliability cuts generated from the probabilistic reliability subproblem in Section III.C are iteratively added. Optimal solutions P^{bc}_{iht} , y_{it} , y_{lt} , and y_{at} are passed on to the two subproblems.

$$\min \left(IC + OC + C^{I} \cdot \sum_{t} \Delta D_{t}^{bc} + C^{W} \cdot \sum_{t} \Delta W_{t}^{bc} \right)$$

s.t. Constraints (2) and (4)-(6)

$$\boldsymbol{L}^{\mathrm{pg}} \left(\frac{P_{iht}^{wc,k}, P_{wht}^{wc,k}, P_{aht}^{wc,k}, D_{dht}^{wc,k}, P_{f,wht}^{wc,k},}{AL_{lht}^{wc,k}, AU_{iht}^{wc,k}, v_{dht}^{+wc,k}, v_{dht}^{-wc,k}} \right) \leq 0$$

$$\Delta D_t^{wc,k} = \sum_h \sum_d DT_{ht} \cdot \left(v_{dht}^{+wc,k} + v_{dht}^{-wc,k} \right)$$

Dual reliability cuts generated so far. (11)

Note that the master problem is a mixed-integer nonlinear programming (MINLP) problem with nonlinear gas flow equation (5.3)-(5.4). We follow the convention to convert (11)into a mixed-integer linear programming (MILP) problem with a better computational performance [32]-[33]. For instance, the nonlinear term $(f_{pht}^+ - f_{pht}^-) \cdot (Pr_{mht} - Pr_{nht})$ in (5.3) can be equivalently represented as in (12) via an auxiliary variable gr_{pht} [34]. Equation (5.4) for candidate lines can be similarly reformulated, with additional constraints (13) to further enforce the relationship between gas flows and pipeline investment decisions. Indeed, the quadratic term Q_{pht}^2 in (13) can be piecewise linearized to derive the final MILP representation [32]-[35], while K_{mn} is the pipeline constant. In [35], three different models for linearizing nonlinear gas flow constraints are compared, including convex combination model, multiplechoice model, and incremental model. It is indicated that the incremental model outperforms the other two techniques via theoretical and computational analysis. Indeed, the most promising advantage of the incremental model is its computational performance for optimizing gas network operations. In the piecewise linearization technique, more segments in the linearization process would derive a better approximation, at the cost of more continuous and binary variables with a higher computational burden.

$$gr_{pht} \ge Pr_{nht} - Pr_{mht} + \left(f_{pht}^{+} - f_{pht}^{-} + 1\right) \cdot \left(Pr_{m}^{l} - Pr_{n}^{u}\right)$$
 (12.1)

$$gr_{pht} \ge Pr_{mht} - Pr_{nht} + \left(f_{pht}^{+} - f_{pht}^{-} - 1\right) \cdot \left(Pr_{m}^{u} - Pr_{n}^{l}\right)$$
 (12.2)

$$gr_{pht} \le Pr_{nht} - Pr_{mht} + \left(f_{pht}^+ - f_{pht}^- + 1\right) \cdot \left(Pr_m^u - Pr_n^l\right)$$
 (12.3)

$$gr_{pht} \le Pr_{mht} - Pr_{nht} + \left(f_{pht}^{+} - f_{pht}^{-} - 1\right) \cdot \left(Pr_{m}^{l} - Pr_{n}^{u}\right)$$
 (12.4)

$$-\left(1-z_{pt}\right)\cdot M \leq gr_{pht}-Q_{pht}^{2}/K_{mn}^{2} \leq \left(1-z_{pt}\right)\cdot M,$$

$$p \in CP$$
 (13.1)

$$-z_{pt} \cdot M \le Q_{pht} \le z_{pt} \cdot M, \qquad p \in \mathbf{CP} \qquad (13.2)$$

B. N-1 Security Subproblem

The N-1 max-min subproblem (8.1)-(8.19) identifies the worst-case realization D_{dht}^{wc} , $P_{f,wht}^{wc}$, AU_{iht}^{wc} and AL_{lht}^{wc} that would lead to the largest possible system load imbalance, with respect to the master solution P_{iht}^{bc} , y_{it} , y_{lt} and y_{at} . This worst-case scenario will be added into the master problem to obtain a new solution that will mitigate the system load imbalance. Note that gas network feasibility constraint (8.20) for individual worst case realizations will be checked in the master problem, instead of this subproblem. Thus, with an inner linear programming model, the max-min subproblem (8.1)-(8.19) can be converted into a single-level bilinear optimization problem (14).

$$\begin{split} &\Delta D_{t}^{wc} = \max \sum_{h \ d \in N(b)} \sum_{dht}^{D} \cdot \beta_{bht} + \sum_{h \ l \in CL} \left(1 - \hat{y}_{lt} \cdot AL_{lht}\right) \cdot M \cdot \gamma_{lht} \\ &+ \sum_{h \ l \in CL} \left(1 - \hat{y}_{lt} \cdot AL_{lht}\right) \cdot M \cdot \eta_{lht} + \sum_{h \ l \in EL} \sum_{l \in EL} PL_{l}^{\max} \cdot \left(\hat{\lambda}_{lht} + \mu_{lht}\right) \\ &+ \sum_{h \ l \in CL} \sum_{l \in CL} Pl_{l}^{\max} \cdot \hat{y}_{lt} \cdot AL_{lht} \cdot \left(\pi_{lht} + \delta_{lht}\right) + \sum_{h \ b} \mathcal{D}_{b}^{\max} \cdot \left(\alpha_{bht} + \varepsilon_{bht}\right) \\ &+ \sum_{h \ l \in EG} \sum_{l \in CL} P_{l}^{\max} \cdot \hat{y}_{lt}^{retire} \cdot \sigma_{lht} + \sum_{h \ l \in CG} P_{l}^{\max} \cdot \hat{y}_{it} \cdot \tilde{\varepsilon}_{lht} \\ &+ \sum_{h \ l \in EG} \sum_{l \in CA} P_{l}^{\max} \cdot \mathcal{C}_{aht} + \sum_{h \ l \in CG} P_{l}^{\max} \cdot \hat{y}_{at} \cdot \mathcal{D}_{aht} \\ &+ \sum_{h \ l \in EA} \sum_{l \in CA} P_{l}^{\max} \cdot \mathcal{C}_{aht} + \sum_{h \ l \in CA} P_{l}^{\max} \cdot \hat{y}_{at} \cdot \mathcal{D}_{aht} \\ &+ \sum_{h \ l \in EA} \sum_{l \in CA} P_{l}^{\max} \cdot \mathcal{C}_{aht} + \sum_{h \ l \in CG} P_{l}^{\max} \cdot \hat{y}_{at} \cdot \mathcal{D}_{aht} \\ &+ \sum_{h \ l \in EA} \sum_{l \in CA} P_{l}^{\max} \cdot \mathcal{C}_{aht} + \sum_{h \ l \in CG} P_{l}^{\max} \cdot \hat{y}_{at} \cdot \mathcal{D}_{aht} \\ &+ \sum_{h \ l \in EA} \sum_{l \in CA} P_{l}^{\max} \cdot \mathcal{C}_{aht} + \sum_{h \ l \in CA} P_{l}^{\max} \cdot \hat{y}_{at} \cdot \mathcal{D}_{aht} \\ &+ \sum_{h \ l \in EA} P_{l}^{\max} \cdot \mathcal{C}_{aht} + \mathcal{C}_{l} \cdot \mathcal{C}_{l}^{\max} \cdot \hat{y}_{at} \cdot \mathcal{D}_{aht} \\ &+ \sum_{h \ l \in EA} P_{l}^{\max} \cdot \mathcal{C}_{aht} + \mathcal{C}_{l}^{\max} \cdot \mathcal{C}_{aht} + \sum_{h \ l \in CG} P_{l}^{\max} \cdot \hat{y}_{at} \cdot \mathcal{D}_{aht} \\ &+ \sum_{h \ l \in EA} P_{l}^{\max} \cdot \mathcal{C}_{aht} \cdot \mathcal{C}_{aht} + \mathcal{C}_{l}^{\max} \cdot \hat{y}_{at} \cdot \mathcal{D}_{aht} \\ &+ \sum_{h \ l \in EA} P_{l}^{\max} \cdot \mathcal{C}_{aht}^{\max} \cdot \mathcal{C}_{aht}^{\max} \cdot \hat{y}_{at} \cdot \mathcal{D}_{aht} \\ &+ \sum_{h \ l \in EA} P_{l}^{\max} \cdot \mathcal{C}_{aht}^{\max} \cdot \mathcal{C}_{aht}^{\max} \cdot \hat{y}_{at}^{\max} \cdot \hat{y}_{at}^{\min} \cdot \hat{y}_{at}^{\max} \cdot \hat{y}_{at}^{\max} \cdot \hat{y}_{at}^{\min} \cdot \hat{y}_{at$$

The objective function of (14) includes bilinear terms, i.e., products of two continuous variables (i.e., an uncertainty variable and a dual variable) and products of a binary variable and a dual variable. The product of an uncertainty variable and a dual variable can be linearized via auxiliary binary variables together with extreme values of uncertainty variables, because in the worst case a continuous uncertainty variable D^u_{dht} always takes its upper/lower limit or the forecasted value [36]. For instance, bilinear term $D^u_{dht} \cdot \beta_{bht}$ can be linearized as in (15),

where cc_{bht}^0 , cc_{bht}^+ and cc_{bht}^- are auxiliary binary variables. On the other hand, the product of a binary variable and a dual variable can be linearized using the well-known algebra results. For example, bilinear term $AL_{lht} \cdot \gamma_{lht}$ can be linearized as in (16).

$$D_{dht}^{u} \cdot \beta_{bht} = D_{dht}^{bc} \cdot \beta_{bht}^{0} + \left(D_{dht}^{bc} + \tilde{D}_{dht}\right) \cdot \beta_{bht}^{+} + \left(D_{dht}^{bc} - \tilde{D}_{dht}\right) \cdot \beta_{bht}^{-}, d \in N(b)$$

$$(15.1)$$

$$\beta_{bht} = \beta_{bht}^0 + \beta_{bht}^+ + \beta_{bht}^- \tag{15.2}$$

$$cc_{bht}^{0} + cc_{bht}^{+} + cc_{bht}^{-} = 1 (15.3)$$

$$-cc_{bht}^0 \cdot M \le \beta_{bht}^0 \le cc_{bht}^0 \cdot M \tag{15.4}$$

$$-cc_{bht}^+ \cdot M \le \beta_{bht}^+ \le cc_{bht}^+ \cdot M \tag{15.5}$$

$$-cc_{bht}^{-} \cdot M \le \beta_{bht}^{-} \le cc_{bht}^{-} \cdot M \tag{15.6}$$

$$rr_{lht} = AL_{lht} \cdot \gamma_{lht} \tag{16.1}$$

$$-AL_{lht} \cdot M \le rr_{lht} \le 0 \tag{16.2}$$

$$\gamma_{lht} - (1 - AL_{lht}) \cdot M \le rr_{lht} \le \gamma_{lht} + (1 - AL_{lht}) \cdot M \tag{16.3}$$

With above linearization approaches, the bilinear subproblem (14) can be reformulated as an MILP problem and solved by commercial MILP solvers.

C. Probabilistic Reliability Subproblem

The probabilistic reliability subproblem evaluates system reliability level (3) with respect to random outages of generators and transmission lines. The LOLE index has been widely accepted and used in power industry to evaluate the overall reliability of power systems [16], [25]-[26], which quantifies the number of days in a year that electrical loads cannot be sufficiently supplied. This metric does not provide information on the potential total energy shortfall. Usually, the standard LOLE level in power industry is 0.1day/year or one day in ten years. Following the practice in power industry, the proposed model adopts the LOLE index (3) to evaluate the reliability of power systems. As the annual wind power generation profile of a certain location usually remains unaltered from year to year [37], short-term load and wind power uncertainties are addressed in the security operation subproblem instead. That is, the LOLE index will reflect the long-term overall reliability of the system over a long period of time (say one year), and the operating security of the system is guaranteed by the N-1 security subproblem.

In this paper, Latin Hypercube Sampling based Monte Carlo (MC) simulation is adopted to estimate system LOLE with forced outage rates of system components [38]. The reliability checking subproblem for the qth MC sample of load block h in year t is given in (17). The MC simulation stops when coefficient of variation is less than 1% [38]. Finally, the system LOLE for each year t can be calculated as in (18) using solutions to all NS MC sample subproblems, where $1_{\varepsilon} \left(ENS_{ht} \right)$ is an indicator function with the value of 1 if $ENS_{ht,q}$ is no smaller than a smaller threshold ε and otherwise 0. If the reliability criterion (3) is not satisfied, a dual reliability

cut (19) will be generated and incorporated into the master problem.

$$\begin{aligned} &\min ENS_{ht}^{q} = \sum_{d} DT_{ht} \cdot \left(v_{dht}^{+mc,q} + v_{dht}^{-mc,q}\right) \\ &\text{s.t.} \\ &\sum_{i \in N(b)} P_{iht}^{mc,q} + \sum_{w \in N(b)} P_{wht}^{mc,q} - \sum_{s(l) \in N(b)} PL_{lht}^{mc,q} + \sum_{r(l) \in N(b)} PL_{lht}^{mc,q} \\ &- \sum_{a \in N(b)} P_{aht}^{mc,q} + \sum_{d \in N(b)} \left(v_{dht}^{+mc,q} - v_{dht}^{-mc,q}\right) = \sum_{d \in N(b)} D_{dht}^{bc} \\ &PL_{lht}^{mc,q} \cdot X_{l} = AL_{lht}^{mc,q} \cdot \left(\theta_{s(l)ht}^{mc,q} - \theta_{r(l)ht}^{mc,q}\right), \quad l \in EL \\ &- \left(1 - \hat{y}_{lt} \cdot AL_{lht}^{mc,q}\right) \cdot M \leq PL_{lht}^{mc,q} \cdot X_{l} - \left(\theta_{s(l)ht}^{mc,q} - \theta_{r(l)ht}^{mc,q}\right) \\ &\leq \left(1 - \hat{y}_{lt} \cdot AL_{lht}^{mc,q}\right) \cdot M, l \in CL : \left(\mathcal{G}_{lht}^{2,q}, \mathcal{G}_{lht}^{1,q}\right) \\ &- PL_{l}^{\max} \leq PL_{lht}^{mc,q} \leq PL_{lht}^{\max}, \quad l \in EL \\ &- PL_{l}^{\max} \cdot \hat{y}_{lt} \cdot AL_{lht}^{mc,q} \leq PL_{lht}^{mc,q} \leq PL_{lht}^{\max} \cdot \hat{y}_{lt} \cdot AL_{lht}^{mc,q}, \\ &- PL_{lht}^{\max} \cdot \hat{y}_{lt} \cdot AL_{lht}^{mc,q} \leq PL_{lht}^{\max}, \quad l \in EG \\ &0 \leq P_{iht}^{mc,q} \leq P_{i}^{\max} \cdot \hat{y}_{it} \cdot AU_{iht}^{mc,q}, \quad i \in EG \\ &0 \leq P_{iht}^{mc,q} \leq P_{i}^{\max} \cdot \hat{y}_{it} \cdot AU_{iht}^{mc,q}, \quad i \in EG \\ &0 \leq P_{aht}^{mc,q} \leq P_{a}^{\max}, \quad i \in EA \\ &0 \leq P_{aht}^{mc,q} \leq P_{a}^{\max}, \quad i \in EA \\ &0 \leq P_{aht}^{mc,q} \leq P_{a}^{\max}, \quad i \in EA \\ &0 \leq P_{wht}^{mc,q} \leq P_{i,wht}^{mc}, \quad l \in EA \\ &0 \leq P_{wht}^{mc,q} \leq P_{i,wht}^{mc}, \quad l \in EA \\ &0 \leq P_{wht}^{mc,q} \leq P_{i,wht}^{mc}, \quad l \in EA \\ &0 \leq P_{wht}^{mc,q} \leq P_{i,wht}^{loc}, \quad l \in EA \\ &0 \leq P_{wht}^{mc,q} \leq P_{i,wht}^{loc}, \quad l \in EA \\ &0 \leq P_{iht}^{mc,q} \leq P_{i,wht}^{loc}, \quad l \in EA \\ &0 \leq P_{iht}^{mc,q} \leq P_{i,wht}^{loc}, \quad l \in EA \\ &0 \leq P_{iht}^{mc,q} \leq P_{i,wht}^{loc}, \quad l \in EA \\ &0 \leq P_{iht}^{mc,q} \leq P_{i,wht}^{loc}, \quad l \in EA \\ &0 \leq P_{iht}^{mc,q} \leq P_{i,wht}^{loc}, \quad l \in EA \\ &0 \leq P_{iht}^{mc,q} \leq P_{i,wht}^{loc}, \quad l \in EA \\ &0 \leq P_{iht}^{mc,q} \leq P_{i,wht}^{loc}, \quad l \in EA \\ &0 \leq P_{iht}^{mc,q} \leq P_{i,wht}^{loc}, \quad l \in EA \\ &0 \leq P_{iht}^{mc,q} \leq P_{i,wht}^{loc}, \quad l \in EA \\ &0 \leq P_{iht}^{mc,q} \leq P_{i,wht}^{loc}, \quad l \in EA \\ &0 \leq P_{iht}^{mc,q} \leq P_{i,wht}^{loc}, \quad l \in EA \\ &0 \leq P_{iht}^{mc,q} \leq P_{i,wht}^{loc}, \quad l \in EA \\ &0 \leq P_{iht}^{mc,q} \leq P_{i,wht}^{loc}$$

As annual system LOLE is a probabilistic index which depends on investment and operation decisions, explicit analytical formula for (3) is not readily available. Alternatively, the reliability checking subproblem (17) calculates potential load shedding quantities among multiple scenarios, and consequently the LOLE index is post-calculated as in (18) to evaluate system reliability. However, as LOLE is not explicitly treated as a decision variable in (17), the LOLE index cannot be directly used to generate reliability cuts, while a dual reliability cut (19) with respect to EENS is used when the LOLE criterion is not met. Indeed, as Benders decomposition is an exact algorithm which guarantees solution optimality decomposition [10], [17], dual reliability cuts generated via dual solutions of the reliability checking subproblem (17) represent valid cutting planes that can mitigate load shedding by optimally adjusting planning decisions in the master problem. The same strategy has also been adopted in [10], [17],

[37].

It is also noted that optimal planning decisions derived via the EENS based dual reliability cut (19) could be different from the LOLE index directly, while the proper setting on EENS^{max} in (19) could help mitigate such difference. For instance, reference [39] provides a way to set EENS^{max} according to electrical load levels. For example, in case studies of this paper, EENS^{max} can be set as 3% percent of the peak load (i.e., 2850 MW) which yields 205MWh (i.e., 0.1*24*2850*0.03 with respect to the LOLE threshold of 0.1day/year). In practice, in order to ensure that the final optimal planning decisions derived from the dual reliability cut (19) are as close to those of the LOLE index as possible, decision makers can dynamically adjust EENS^{max} via an iterative procedure. That is, a relatively large EENS^{max}, saying 5% of the peak load, can be used in the first few iterations, if the LOLE criterion is not met while the EENS^{max} is satisfied, EENS^{max} can be gradually reduced in later iterations until the LOLE criterion (18) is satisfied.

In this paper, both N-1 criterion and probabilistic reliability criterion are adopted for evaluating co-optimization planning decisions in two distinct subproblems. The max-min N-1 security checking subproblem is formulated as a robust optimization model, which simulates wind power uncertainties via an uncertainty set (8.4). In comparison, concerning stochastic nature of renewable energy, the approach discussed in [40] calculates reliability indices with pre-calculated deliverable capacity probability table (DCPT) and available capacity probability table (ACPT). However, this technique cannot be directly applied in the proposed robust optimization based approach, because it only quantifies reliability performance of certain planning decisions but does not presents strategies on how planning decisions could be adjusted to further improve system reliability. In addition, [41]-[43] use sequential Monte Carlo simulation to sample uncertain wind power scenarios via the ARMA model, which are integrated in a stochastic programming framework to determine optimal operations of power systems. In other words, the sequential Monte Carlo Simulation, which generates multiple scenarios to simulate random outages of generators/transmission lines and uncertain loads/wind generations in stochastic programming, is not suitable for the proposed robust optimization based approach which is based on the uncertainty set. Furthermore, in the max-min N-1 security checking subproblem, a sequential model with 8760-hour time-series data may be computationally intractable, because its equivalent single-level bilinear optimization problem (14) will include a significant number of binary variables indicating outage statuses of generators/ transmission lines and uncertainty levels of loads/wind generations. It is noted that the single-level bilinear optimization problem (14) needs to be equivalently converted into a mixed-integer linear programming problem for the solution, which will introduce additional binary variables and further complicate the computation. In turn, we follow the convention of robust optimization-based power system planning in literature [28], [37], [44]-[45], to use several load blocks instead of the 8760-hour time-series data.

In addition, the probabilistic reliability subproblem

evaluates system reliability level with respect to random outages of generators and transmission lines, while neglecting uncertainties of renewable energy and loads. To keep consistency of the two subproblems, the probabilistic reliability subproblem also adopts load blocks. Consequently, a Latin Hypercube Sampling based Monte Carlo simulation, instead of the sequential Monte Carlo simulation, is used to sample random outages of generators and transmission lines in each load block for calculating LOLE index. Furthermore, optimization-based planning approaches in [10]-[11], [37] also adopt load blocks as a trade-off between computational efficiency and solution accuracy to evaluate system reliability.

D. Implementation of the Algorithm

The solution procedure is as follows.

- Step 1) Set thresholds for base-case load shedding $\Delta D_t^{bc,\text{max}}$ and worst-case system power imbalance $\Delta D_t^{wc,\text{max}}$ Initialize iteration counters k=1 and r=1.
- Step 2) Solve the master problem (11), and pass the optimal solution \hat{P}_{iht}^{bc} , \hat{y}_{it} , \hat{y}_{lt} and \hat{y}_{at} to Step 3.
- Solve the N-1 security subproblem (14) with respect to \hat{P}^{bc}_{iht} , \hat{y}_{it} , \hat{y}_{lt} and \hat{y}_{at} , and identify the worst-case realization $D^{wc,k}_{dht}$, $P^{wc,k}_{f,wht}$, $AU^{wc,k}_{iht}$ and $AL^{wc,k}_{lht}$ that leads to the largest possible system power imbalance. If the annual largest possible security violation is smaller than $\Delta D^{wc,\max}_{t}$, go to Step 4; Otherwise, add the worst case $D^{wc,k}_{dht}$, $P^{wc,k}_{f,wht}$, $AU^{wc,k}_{iht}$ and $AL^{wc,k}_{lht}$ into the master problem (11), set k=k+1, and go to Step 2
- Step 4) Solve the probabilistic reliability subproblem (17) with respect to investment decisions \hat{y}_{it}^r and \hat{y}_{lt}^r , and calculate the annual $LOLE_t(18)$. If the annual $LOLE_t$ is smaller than $LOLE^{\max}$, Terminate; Otherwise, add dual reliability cut (19) to the master problem (11), set r=r+1, and go to Step 2.

IV. CASE STUDIES

In this section, the modified 24-bus IEEE Reliability Test System (RTS) [46] and a 12-node gas system [47] is first used to demonstrate the effectiveness of the proposed co-optimization planning approach via numerical comparisons with other alternatives. A larger system, consisting the modified IEEE 118-bus power system and the Belgian high-calorific 20-nodel natural gas system, is further studied to evaluate its computational performance. Cost coefficients of electrical load imbalance C^I and wind spillage C^W are set as \$106/MWh [48] and \$100/MWh [49], respectively.

All case studies are solved on a Dell work station with two Intel Xeon E5-2620 processors at 2.1 GHz and 64 GB memory, and Gurobi 6.5 is used as the MILP solver. The incremental model [32]-[35] with two segments is adopted to linearize the Weymouth equation as a tradeoff between computational

efficiency and solution accuracy. Normally, the big-M should be large enough to make sure that the reformulated constraints are valid. However, a too-large big-M may deteriorate the computational performance. Specifically, in this paper, magnitudes of power flows, gas flows, and squared gas pressure differences are all smaller than 10⁵. In addition, for unbounded dual variables (15)-(16), reference [50] has tested the performance of different values of big-M and concluded that the ideal range is [10⁴, 10⁶] for ensuring a good computational efficiency. Thus, the big-M is set as 10⁶ in all case studies.

A. The modified 24-bus IEEE RTS and a 12-node gas system

The modified 24-bus IEEE RTS includes 19 non-gas and 7 gas units, 3 wind farms, 38 lines, and 17 electrical loads. 18 candidate units with 9 being gas, 16 candidate lines, and 3 candidate PtGs are considered. The gas system includes 3 gas suppliers, 10 pipelines, and 8 non-power gas loads as shown in Fig. 1. Candidate assets include 3 gas wells, 2 compressor stations, and 10 pipelines. Discount rate is 5%. The optimality gap is set as 0.01%. Other configuration data can be found in [51].

A 10-year planning horizon is studied, with 4 load blocks in each year. Electrical load, wind power, and non-power gas load in the first planning year are 2850MW, 720MW, and 10000kcf/h with average growth rates of 3%, 8%, and 5%. The 4-block load duration curve and wind profile used in case studies are shown in Fig. 2, which are derived based on actual ERCOT data in year 2014 [52] via the k-means algorithm [53]. Fig. 2 shows that characteristics of load/wind and their correlations are partially kept in the 4-block curves. Specifically, the first block of an 87-hour duration represents a high-load/low-wind situation, and the last block of a 3408-hour duration reflects a low-load/high-wind situation. Indeed, these two situations represent the two most critical operation statuses of power systems, which usually have a higher impact on system reliability.

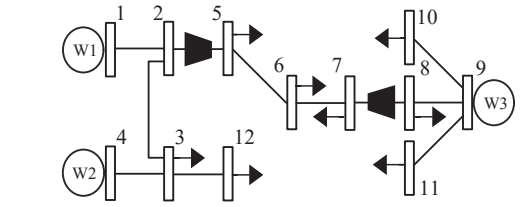


Fig. 1 A 12-node natural gas system.

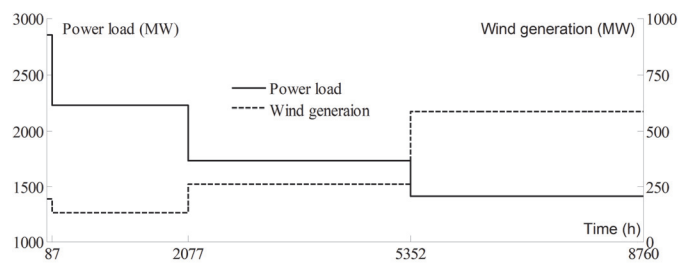


Fig. 2 4-block load duration curve and wind profile

A1. Advantage of Co-Optimization Planning Approach

This section demonstrates advantages of the proposed

co-optimization planning approach via three cases:

- Case 1: Sequential planning of the two systems
- Case 2: Co-optimization planning of interdependent systems
- Case 3: Co-optimization planning while considering retirement of existing coal-fired units

Table I shows results of Cases 1-3, in which the two subscripts represent indices of candidate assets and installation years. For the sake of comparison, power system uncertainties are not considered in these cases. In Case 1, electricity and gas systems are planned sequentially with a total cost of 4.1905 B\$. That is, power system planning is first executed while ignoring gas network characters, and gas system expansion is optimized with fixed planning decisions of power systems (e.g., gas units and PtGs). When co-optimization is considered in Case 2, the total cost is reduced to 4.1476 B\$. The reason is that in the sequential planning process of Case 1, cheaper gas-fired units like G4 and G14 are invested earlier while neglecting limited gas delivery capability of the existing gas network. As a result, the gas network has to invest in pipelines and compressor stations more extensively and earlier. In contrary, the co-optimization planning in Case 2 considers gas network costs and limitations in the power system planning stage, and in turn more economical investment decisions can be achieved.

In Case 3, retirement of existing coal-fired units is further considered, i.e., by the end of the planning year, 5 units with a total capacity of 372MW will be retired. In turn, as compared to Case 2, two more gas units G6 and G16 are constructed to replace the retired coal-fired units and meet increased electrical loads. Consequently, pipeline P10 is constructed to ensure sufficient natural gas supply to newly-built gas units.

In order to show the importance and advantage of PtGs and compressor stations in the interdependent systems, two cases are further carried out: Case 3 without PtGs (i.e., Case 3.1) and Case 3 without compressor stations (i.e., Case 3.2). As shown in Table II, in Case 3.1, due to the lack of PtG facility A1 to economically convert excessive wind energy into natural gas, transmission lines L3 and L9 have to be constructed to effectively utilize growing wind energy and prevent wind spillage, which almost triples the investment cost. In Case 3.2, as compressor station C1 is not installed, two pipelines P1 and P8 are respectively constructed in years 5 and 10 to ensure gas delivery capability to newly-built gas units with a much higher investment cost. These two cases show that PtGs and gas compressors provide a more economical way to effectively support the growing penetration of wind energy and gas units.

TABLE I COMPARISON OF AMONG CASES 1-3

Case	Constructed components	Total cost (B\$)
1	$G_{1,3},G_{3,7},G_{4,8},G_{11,10},G_{13,9},G_{14,4},G_{15,6},\ A_{1,9},S_{3,5},P_{3,2},P_{4,4},P_{10,3},C_{1,3},C_{2,10}$	4.1905
2	$G_{1,3},G_{3,6},G_{4,10},G_{11,5},G_{13,9},G_{14,7},G_{15,4},\ A_{1,9},S_{3,6},P_{3,4},P_{4,7},C_{1,5}$	4.1476
3	$G_{1,3},G_{3,7},G_{4,7},G_{6,9},G_{8,10},G_{11,5},G_{13,9},G_{14,6},G_{15,4},\\G_{16,8},A_{1,9},S_{3,6},P_{3,4},P_{4,7},P_{10,8},C_{1,5}$	4.2960

TABLE II
RESULTS OF CASES 3.1-3.2 AS COMPARED TO CASE 3

Case	Changes in investment decision	Changes in investment cost (M\$)
3.1	$A_{1,9} \rightarrow L_{3,9}, L_{9,10}$	$3.3036 \rightarrow 10.3692$
3.2	$C_{1,5} \rightarrow P_{1,5}, P_{8,10}$	$4.3846 \rightarrow 14.9076$

A2. Advantage of Robust Planning with the Joint Criterion

This section illustrates effectiveness of the robust planning model with wind power recourse cost to mitigate wind spillage under uncertainties as well as advantage of the joint N-1 and probabilistic reliability criterion in providing economical and reliable co-optimization expansion decisions via two cases:

- Case 4: Robust co-optimization planning with uncertainties.
- Case 5: Case 4 with the joint N-1 and probabilistic criterion.

Case 4: This case evaluates the impact of electrical load and wind generation uncertainty on co-optimization planning via the robust optimization approach. Uncertainty intervals of electrical loads and wind generations are set as 5% and 20% of their forecast values. Uncertainty budgets Δ_{dt} and Δ_{wt} are both set as 4. Because all case studies use 4 load blocks in each year, the uncertainty budget is set as the largest value of 4 to maximize the system's ability for handling uncertainties. System power imbalance thresholds $\Delta D_t^{bc, \rm max}$ and $\Delta D_t^{wc, \rm max}$ are both set as 0.01MW to ensure secure operation without load shedding when contingencies are not considered.

Table III shows robust co-optimization planning results with respect to different wind power recourse cost values, including base/ worst case costs, incremental base-worst cost ratio (ICR), and investment statuses of PtG facility A1 and transmission line L3 that are connected to a wind farm. ICR is calculated as the decrease in base-case cost over the increase in worst-case cost for a certain value C^{re} as compared to C^{re} =\$0. It can be observed that as a higher C^{re} allows more wind spillage, base-case cost decreases because certain constructions such as A1 and L3 are delayed or avoided. On the other hand, worst case cost increases because of a high wind spillage penalty cost. In addition, the lowest base-case cost and the highest worst-case cost are both reached when Cre is 40 M\$, which indicates that the recourse cost is not binding anymore and a further increase in C^{re} will not postpone constructions of PtGs or transmission lines. As shown in Table III, when C^{re} is set as 0 which does not allow wind spillage, the co-optimization planning solution could be over-conservative in terms that PtG facility A1 and transmission line L3 are invested much earlier with the highest base-case cost. In comparison, setting the wind power recourse cost as certain values from 10M\$ to 50M\$, less conservative options could be available to decision makers. Specifically, C^{re}=10M\$ is considered as a better wind power recourse cost threshold in this case because of its relatively larger ICR as compared to other C^{re} values, i.e., its base case cost decreases more significantly with a limited increase in worst-case cost. In this case, the base-case cost decreases about 0.45% (19.7M\$) as compared to Cre=\$0, while worst-case cost only increases by 0.2% (9M\$). That is, the optimal planning strategy with C^{re}=10M\$ could effectively reduce the base-case total cost, while only slightly increases the worst-case operation cost when extremely rare situations occur.

Investment details with $C^{\text{re}}=10\text{M}$ \$ are further shown in Table IV. As compared to Case 3, when load and wind uncertainties are considered, constructions of gas units G1, G4, G14, and G15 are delayed, while a large coal unit G13 is constructed much earlier from year 9 in Case 3 to year 3 in this case. The

reason is that gas-fired units G1, G4, G14 and G15 as a whole would lead to gas network congestion in worst-case scenarios, and in turn their constructions require extensive investments in new pipelines in the same year. This would lead to expensive over-investment in the gas network for handling rare worst-case scenarios. Alternatively, the power system seeks for other options (i.e., coal unit G13) to economically meet electrical loads and postpone the construction of gas units and associated expensive pipelines.

As robust optimization and stochastic programming have been recognized as two effective approaches for handling uncertainties in optimization problems, solutions of the proposed robust model is further compared with the stochastic programming model [54]-[55]. In the stochastic programming model, the simulated electrical load and wind power scenarios are assumed to follow uniform distributions within the uncertainty set. 5000 scenarios of 10-year electrical loads and wind generations are generated via the Latin Hypercube sampling method. The number of reduced scenarios is chosen to be 5 as a trade-off between computational speed and solution quality [54]-[55], and these 5 scenarios are directly added in the master problem in Section III.A to obtain the final optimal planning solution. Results of stochastic optimization with C^{re}=10M\$ are reported in Table III, and investment details are presented in Table IV as Case 4.1. It is observed in Tables III-IV that the stochastic programming model yield a smaller total cost for covering high-probability scenarios, while its electricity system planning decision is slightly different from that of the proposed robust optimization approach. However, the stochastic programming planning solution could lead to much higher system load shedding when low-probability high-impact worst case occurs. Indeed, the worst case cost of 5.3644B\$ in the stochastic programming solution is 19.73% higher than that of the robust optimization solution.

TABLE III
SENSITIVITY ANALYSIS WITH DIFFERENT RECOURSE COSTS

SENSITIVITI ANALTSIS WITH DIFFERENT RECOURSE COSTS						
C ^{re} (M\$)	Base-case cost(B\$)	Worst-case cost(B\$)	ICR	A1 (year)	L3 (year)	
0	4.4131	4.4711	0	6	8	
10	4.3934	4.4801	2.1889	7	9	
20	4.3932	4.4811	1.9900	7	9	
30	4.3864	4.5292	0.4596	8	10	
40	4.3847	4.5522	0.3502	9	-	
50	4.3847	4.5522	0.3502	9	-	
stochastic	4.3292	5.3644	0.0939	3	_	

TABLE IV COMPARISON OF CASES 4 AND 5 WITH C^{re} =\$10M

Case	Constructed components	Total cost (B\$)
4	$G_{1,4}, G_{3,5}, G_{4,9}, G_{6,9}, G_{8,10}, G_{11,9}, G_{13,3}, G_{14,7}, G_{15,6}, G_{16,8}, L_{3,9}, L_{9,10}, A_{1.7}, S_{3,6}, P_{3,4}, P_{4,7}, P_{10,8}, C_{1,5}$	4.3934
4.1	$G_{1,5}, G_{3,7}, G_{4,7}, G_{6,9}, G_{8,10}, G_{11,3}, G_{13,9}, G_{14,6}, G_{15,4}, G_{16.8}, L_{10,7}, A_{1,3}, S_{3,6}, P_{3,4}, P_{4,7}, P_{10.8}, C_{1,5}$	4.3292
5	$\begin{array}{l} G_{1,5},G_{3,9},G_{4,9},G_{6,10},G_{8,10},G_{11,1},G_{12,2}G_{13,3},G_{14,7},\\ G_{15,6},G_{16,8},L_{2,9},L_{3,2},L_{5,7},L_{10,9},L_{11,3},L_{15,6},A_{1,4},\\ S_{3,6},P_{3,4},P_{4,7},P_{10,8},C_{1,5} \end{array}$	4.7305

Case 5: This case demonstrates advantage of the proposed joint N-1 and probabilistic reliability criterion, with the same uncertainty settings as in Case 4 and $C^{\text{re}}=10\text{M}$ \$. Since N-1 contingency is considered, $\Delta D_t^{wc,\text{max}}$ is set as 10000MWh to

allow power imbalance under worst-case scenarios. Annual probabilistic reliability criterion *LOLE*^{max} is 0.1day/year, and *EENS*^{max} is set to 3% of annual peak load [39] which yields 205 MWh (i.e., 0.1*24*2850*0.03) in the first year. Investment results of Case 5 are also shown in Table IV. As compared to Case 4, Case 5 derives a higher investment cost with one more generator and six more transmission lines to meet the joint N-1 and probabilistic reliability criterion.

Two more studies with separate N-1 criterion and probabilistic reliability criterion are carried out, to compare with the proposed joint criterion. Results are presented in Table V, and annual LOLEs are further shown in Fig. 3. The 3rd-5th columns of Table V show the total number of transmission lines, units, and generation capacities invested over the ten-year planning horizon. Specifically, N-1 and probabilistic approaches derive very different investment results, while the joint criterion has similar results as the N-1 approach. Indeed, applying N-1 criterion can effectively limit the maximum power imbalance to 10000MWh under worst-case uncertainties and contingencies. However, as shown in Fig. 3, annual LOLEs in years 3-6 are all higher than LOLE^{max} of 0.1day/year. That is, the overall system reliability is not guaranteed. When the probabilistic reliability criterion is employed independently, a lower total cost is obtained while all annual LOLEs are smaller than LOLE^{max}, i.e., system reliability is guaranteed. However, the system could be vulnerable to low-probability/high-impact scenarios. Indeed, the system presents a much higher maximum annual power imbalance of 48770MWh under the worst-case scenario. When N-1 and probabilistic reliability criteria are jointly considered, a compromising result is obtained to limit power imbalance of low-probability/high-damage worst case within 10000MWh and guarantee annual LOLEs lower than 0.1day/year, with a slightly higher total cost than N-1 only.

The proposed joint criterion model is further tested with different power imbalance levels. As shown in Table VI, the total cost decreases with the increase in $\Delta D_t^{wc, \rm max}$, because more power imbalance is allowed and certain investments can be avoided. Specifically, the highest total cost is achieved with $\Delta D_t^{wc, \rm max} = 0$, as more generation capacities are needed for handling contingencies when load shedding is not allowed. However, as both maximum and average annual LOLEs of 0.0645days/year and 0.037days/year are much smaller than $LOLE^{\rm max}$ of 0.1day/year, over-investment would occur when load shedding is not allowed under worst-case contingencies.

The adjustable robust optimization planning model proposed in this paper allows decision makers to set the expected load imbalance limit $\Delta D_t^{wc, \rm max}$ under the worst case scenarios, which could result in different investment decisions with different system reliability performance as shown in Table VI. In the proposed planning model, N-1 and probabilistic reliability criteria have to be satisfied simultaneously. As discussed above, conservativeness of the N-1 criterion can be adjusted by setting different values of the worst-case load imbalance limit $\Delta D_t^{wc, \rm max}$. As observed from Table VI, a

smaller N-1 load imbalance limit $\Delta D_t^{wc, \max}$ could enhance system reliability with a higher total cost. On the other hand, as indicated in Table V, when the probabilistic reliability criterion is employed only, the system reliability can be guaranteed in terms that all annual LOLEs are smaller than $LOLE^{\max}$. However, the system could be vulnerable to low-probability/high-impact scenarios with a large load imbalance. Thus, by leveraging N-1 and probabilistic reliability criteria within the proposed joint reliability criterion framework, decision makers can set proper values of the worst-case load imbalance limit $\Delta D_t^{wc, \max}$ and the reliability target $LOLE^{\max}$, so that system LOLE requirement with respect to high-probability/low-damage events and the worst-case load imbalance in response to low-probability/high-damage events can be balanced with a low overall cost.

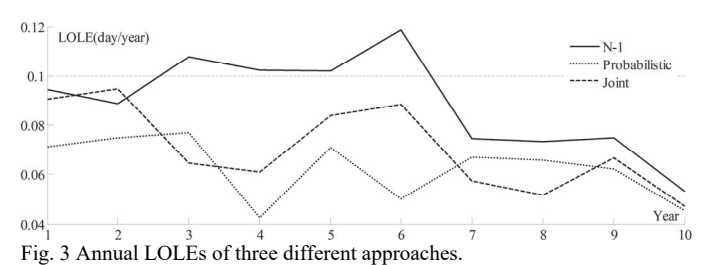


TABLE V

COMPARISON AMONG DIFFERENT RELIABILITY CRITERIA

Approach	Total cost (B\$)	Total lines	Total units	Total capacities (MW)	Maximum power imbalance (MWh)
Joint	4.7305	29	50	5914	10000
N-1	4.7114	29	49	5749	10000
Probabilistic	4.5298	4	52	6238	48770

Δ	$\Delta D_t^{wc, \max}$	Total	Total	Total	Total capacities	$LOLE_t$ (d	ay/year)
	(MWh)	cost (B\$)	lines	units	(MW)	max	mean
	0	4.9872	24	59	6749	0.0645	0.0366
	3000	4.8728	30	57	6518	0.0718	0.0450
	6000	4.7862	30	54	6218	0.0752	0.0512
	10000	4.7305	29	50	5914	0.0948	0.0707

B. The modified IEEE 118-bus power system and the Belgian high-calorific 20-nodel natural gas system

In this section, the proposed approach is further applied to a larger test system for evaluating its computational performance. The test system consists of the modified IEEE 118-bus power system and the Belgian high-calorific 20-nodel natural gas system. Specifically, the test system includes 46 non-gas and 8 gas units, 7 wind farms, 186 lines, 91 electrical loads, 2 gas suppliers, 17 pipelines, 1 compressor station, and 9 non-power gas loads. Candidate assets include 21 generating units with 9 being gas, 15 transmission lines, 3 PtGs, 3 gas wells, 1 compressor station, and 5 pipelines [51]. A 10-year planning horizon is carried out, with 4 load blocks in each year. Peak electrical load, wind power, and non-power gas load in the first planning year are 5400MW, 665MW, and 10000kcf/h, with average annual growth rates of 3%, 8%, and 5%, respectively. The MILP gap is set as 1%. Other parameter settings are the same as the 24-bus RTS study.

The same five cases studied for the 24-bus RTS are explored here, and their computational times are reported in Table VII. Specifically, Case 1 cannot derived a feasible sequential planning strategy, indicating that if all cheaper gas-fired units are constructed in the first step, the natural gas network cannot meet gas requirement of all gas-fired units. In addition, heterogeneous computational performance among multiple cases indicates that high computational cost of the proposed robust co-optimization planning model is dependent on two major factors.

- 1) The sophisticated and realistic natural gas network modeling, including nonlinear Weymouth gas flow equations and rigorous modeling of natural gas compressors. Specifically, (i) linearized Weymouth gas flow equations introduce a large number of binary variables, and gas compressor modeling requires additional binary investment/operation variables as well as big-M constraints. In turn, as compared to the sequential planning strategy of Case 1 which calculates power system planning in 6s, computational time of the co-optimization planning in Case 2 is increased to 60s; (ii) considering compressors further complicates the calculation, as compressors can enhance the transportation capability of existing pipelines by elevating gas nodal pressure levels and consequently could lead to more flexible investment and operation options. As a result, computational time of Case 3 increases significantly to 99s as compared to 59s of Case 3.2 without compressors; (iii) considering retirement of traditional coal-fired units triggers more investments in cheaper gas-fired units, which further intensifies interdependency of the two energy systems and deteriorates the computational performance. Indeed, computational time of Case 3 is increased by about 68% as compared to Case 2.
- 2) Computational burden of the robust optimization approach. As well recognized by [29] and [44]-[45], computational efficiency of the robust optimization approach remains an issue for practical large-scale systems. When uncertainties of electrical loads and wind generations are considered, the running time is increased from 99s in Case 3 to about 369s in Case 4. The joint N-1 and probabilistic criterion in Case 5 requires even longer time because more worst-case contingency scenarios and reliability cuts are generated. However, the running time of about 30 hours for Case 5 would be still acceptable for a practical ten-year planning problem (for instance, it spends several weeks for analyzing a single future scenario in NYISO practice [56]).

TABLE VII
COMPUTATION TIME OF DIFFERENT CASES

Case	Time	Case	Time	Case	Time
1	-	2	60s	3.2	59s
1-power	6s	3	99s	4	369s
1-gas	-	3.1	55s	5	30h

V. CONCLUSION

This paper proposes a long-term robust co-optimization planning model for electricity and gas systems with uncertainties. The proposed model simultaneously optimizes investments of generators, transmission lines, PtGs, gas suppliers, pipelines, and compressor stations. The probabilistic reliability criterion along with the widely accepted N-1 criterion is incorporated to derive reliable and economic co-planning decisions. The proposed model is solved via a decomposition approach, by iteratively solving a master problem and two operation subproblems for checking N-1 and probabilistic reliability criteria.

Simulation results show that: (i) co-optimization planning can reduce the total cost of electricity and gas systems; (ii) the joint N-1 and probabilistic reliability criterion can simultaneously limit the worst-case power imbalance and guarantee the overall system reliability; (iii) investment decisions of the two systems are highly interdependent. For instance, the retirement of coal units would trigger more gas units to be invested, and consequently new pipelines and gas compressors are needed to ensure sufficient gas supply. On the other hand, potential gas network congestion under worst-case scenarios would postpone investment of gas units; (iv) PtGs can facilitate a deeper penetration of wind energy and postpone the construction of transmission lines; (v) compressor stations can enhance gas delivery capacity of the gas network and delay the construction of pipelines; and (vi) wind power recourse cost is a useful index to limit wind spillage under uncertainties, promote PtGs, and utilize more wind energy. In sum, the proposed co-optimization approach could benefit decision makers with useful technique support in interdependent system planning.

REFERENCES

- EIA, Monthly Energy Review, 2016, [Online]. Available: http://www.eia.gov/totalenergy/data/monthly/#naturalgas/.
- [2] M. Götz, J. Lefebvre, F. Mörs, A. Koch, F. Graf, S. Bajohr, R. Reimert and T. Kolb, "Renewable Power-to-Gas: A technological and economic review," *Renewable Energy*, vol. 85, pp. 1371-1390, Jan. 2016.
- [3] G. Gahleitner, "Hydrogen from renewable electricity: An international review of power-to-gas plants for stationary applications," *Int. J. Hydrogen Energy*, vol. 38, no. 5, pp. 2039-2061, 2013.
- [4] Australian Energy Market Operator (AEMO), [Online]. Available: http://www.aemo.com.au/.
- [5] DRAFT Primer for Gas-Electric Modeling in MISO's Phase III Clean Power Plan Study, [Online]. Available: https://www.misoenergy.org/.
- [6] Federal Energy Regulatory Commission (FERC), [Online]. Available: https://www.ferc.gov/industries/electric/indus-act/electric-coord.asp.
- [7] C. Unsihuay-Vila, J. W. Marangon-Lima, A. de Souza, I. Perez-Arriaga, and P. Balestrassi, "A model to long-term, multiarea, multistage, and integrated expansion planning of electricity and natural gas systems," *IEEE Trans. Power Syst.*, vol. 25, no. 2, pp. 1154-1168, May 2010.
- [8] M. Chaudry, N. Jenkins, M. Qadrdan, and J. Wu, "Combined gas and electricity network expansion planning," *Appl. Energy*, vol. 113, pp. 1171-1187, 2014.
- [9] J. Qiu, Z. Y. Dong, J. H. Zhao, K. Meng, Y. Zheng, and D. J. Hill, "Low carbon oriented expansion planning of integrated gas and power systems," *IEEE Trans. Power Syst.*, vol. 30, pp. 1035-1046, 2015.
- [10] X. Zhang, M. Shahidehpour, A. Alabdulwahab, and A. Abusorrah, "Security-constrained co-optimization planning of electricity and natural gas transportation infrastructures," *IEEE Trans. Power Syst.*, vol. 30, no. 6, pp. 2984-2993, Nov. 2015.
- [11] J. Qiu, S. Member, Z. Y. Dong, S. Member, and J. H. Zhao, "Multi-stage flexible expansion co-planning under uncertainties in a combined electricity and gas market," *IEEE Trans. Power Syst.*, vol. 30, no. 4, pp. 2119-2129, Jul. 2015.
- [12] J. Qiu, H. Yang, Z. Y. Dong, J. H. Zhao, K. Meng, F. J. Luo, and K. P. Wong, "A linear programming approach to expansion co-planning in gas and electricity markets," *IEEE Trans. Power Syst.*, vol. 31, no. 5, pp. 3594-3606, Sept. 2016.

- [13] F. Barati, H. Seifi, M. S. Sepasian, A. Nateghi, M. Shafie-khah, and J. P. S. Catalão, "Multi-period integrated framework of generation, transmission, and natural gas grid expansion planning for large-scale systems," *IEEE Trans. Power Syst.*, vol. 30, no. 5, pp. 2527-2537, Sep. 2015.
- [14] R. Chen, A. Cohn, N. Fan, and A. Pinar, "Contingency-risk informed power system design," *IEEE Trans. Power Syst.*, vol. 29, no. 5, pp. 2087-2096, Sept. 2014.
- [15] M. Majidi-Qadikolai and R. Baldick, "Integration of N-1 contingency analysis with systematic transmission capacity expansion planning: ERCOT case study," *IEEE Trans. Power Syst.*, vol. 31, no. 3, pp. 2234-2245, 2016.
- [16] J. Choi, T. Tran, A. A. El-Keib, R. Thomas, H. Oh, and R. Billinton, "A method for transmission system expansion planning considering probabilistic reliability criteria," *IEEE Trans. Power Syst.*, vol. 20, no. 3, pp. 1606-1615, Aug. 2005.
- [17] J. Roh, M. Shahidehpour, and L.Wu, "Market-based generation and transmission planning with uncertainties," *IEEE Trans. Power Syst.*, vol. 24, no. 3, pp. 1587-1598, Aug. 2009.
- [18] J. Aghaei, N. Amjady, A. Baharvandi, and M. Akbari, "Generation and transmission expansion planning: MILP-Based probabilistic model," *IEEE Trans. Power Syst.*, vol. 29, no. 4, pp. 1592-1601, Jul. 2014.
- [19] A. Leite da Silva, L. Rezende, L. Manso, and G. Anders, "Transmission expansion planning: A discussion on reliability and security criteria," in Proc. 2010 IEEE 11th Int. Conf. Probabilistic Methods Applied to Power Systems (PMAPS), pp. 244-251, Jun. 2010.
- [20] R. Billinton, G. Yi, and R. Karki, "Application of a joint deterministic-probabilistic criterion to wind integrated bulk power system planning," IEEE Trans. Power Syst., vol. 25, no. 3, pp. 1384-1392, Aug. 2010.
- [21] H. Park and R. Baldick, "Transmission planning under uncertainties of wind and load: Sequential approximation approach," *IEEE Trans. Power Syst.*, vol. 28, no. 3, pp. 2395-2402, Aug. 2013.
- [22] N. Zhang, C. Kang, D. S. Kirschen, Q. Xia, W. Xi, J. Huang, and Q. Zhang, "Planning pumped storage capacity for wind power integration," *IEEE Trans. Sustain. Energy*, vol. 4, no. 2, pp. 393-401, 2013.
- [23] S. Wu, R. Rios-Mercade, E. Boyd, and L. Scott, "Model relaxation for the fuel cost minimization of steady-state gas pipeline networks," *Math. Comput. Model.*, vol. 31, no. 2-3, pp. 197-220, Jan. 2000.
- [24] H. Ye and Z. Li, "Robust Security-Constrained Unit Commitment and Dispatch With Recourse Cost Requirement," *IEEE Trans. Power Syst.*, vol. 31, no. 5, pp. 3527-3536, Sept. 2016.
- [25] MISO Energy, Loss of Load Expectation (LOLE) Fundamentals, 2015, [Online]. Available: https://www.misoenergy.org/Library/Repository/ Meeting%20Material/Stakeholder/LOLEWG/2015/20150304/20150304 %20LOLEWG%20Item%2002%20LOLE%20Fundamentals.pdf.
- [26] PJM, 2014 PJM Reserve Requirement Study, 2014, [Online]. Available: http://www.pjm.com/~/media/planning/res-adeq/2014-pjm-reserve-requirement-study.ashx.
- [27] R. Billinton and R. Allan, Reliability Assessment of Large Power Systems. Boston, MA: Kluwer, 1988.
- [28] R. Jabr, "Robust transmission network expansion planning with uncertain renewable generation and loads," *IEEE Trans. Power Syst.*, vol. 28, no. 4, pp. 4558-4567, Nov. 2013.
- [29] C. Dai, L. Wu, and H. Wu, "A multi-band uncertainty set based robust SCUC with spatial and temporal budget constraints," *IEEE Trans. Power Syst.*, vol. 31, no. 6, pp. 4988-5000, Nov. 2016.
- [30] E. S. Menon, Gas Pipeline Hydraulics. Boca Raton, FL, USA: Taylor & Francis, 2005.
- [31] A. Tomasgard, F. Rømo, M. Fodstad, and K. Midthun, "Optimization models for the natural gas value chain," *Geom. Model., Numer. Simul.*, *Optimiz.*, pp. 521-558, 2007.
- [32] C. He, L. Wu, T. Liu, and M. Shahidehpour, "Robust co-optimization scheduling of electricity and natural gas systems via admm," *IEEE Trans. Sustain. Ener.*, vol. 8, no. 2, pp. 1010-1020, Apr. 2017.
- [33] B. Geißler, A. Martin, A. Morsi, and L. Schewe, "Using piecewise linear functions for solving MINLPs," *Mixed Integer Nonlinear Programming*, pp. 287-314, Springer New York, 2012.
- [34] G. McCormick, "Computability of global solutions to factorable nonconvex programs: Part I-Convex underestimating problems," *Math. Program.*, vol. 10, no. 1, pp. 147-175, 1976.
- [35] C. Correa-Posada and P. Sanchez-Martion. (2014) Gas network optimization: A comparison of piecewise linear models. [Online]. Available: http://www.optimization-online.org/DB FILE/2014/10/4580. pdf.
- [36] D. White, "A linear programming approach to solving bilinear

- programmes," Math. Program., vol. 56, no. 1-3, pp. 45-50, 1992.
- [37] S. Dehghan, N. Amjady, and A. Conejo, "Reliability-Constrained Robust Power System Expansion Planning," *IEEE Trans. Power Syst.*, vol. 31, no. 3, pp. 2383-2392, May 2016.
- [38] R. Billinton and W. Li, Reliability Assessment of Electrical Power Systems Using Monte Carlo Methods, New York: Plenum, 1994.
- [39] A. Liu, B. Hobbs, J. Ho, J. McCalley, Venkat Krishnan, M. Shahidehpour and Q. Zheng "Co-optimization of transmission and other supply resources," Nat. Assoc. Regulatory Utility Commiss., Washington, DC, USA, Sept. 2013.
- [40] A. Mehrtash, P. Wang, and G. Goel, "Reliability evaluation of power systems considering restructuring and renewable generators," *IEEE Trans. Power Syst.*, vol. 27, no. 1, pp. 243-247, Sept. 2014.
- [41] R. Billinton, R. Karki, G. Yi, H. Dange, H. Po, and W. Wangdee, "Adequacy assessment considerations in wind integrated power systems," *IEEE Trans. Power Syst.*, vol. 27, no. 4, pp. 2297-2305, Nov. 2012.
- [42] R. Xiao, Y. Xiang, L, Wang and K. Xie, "Bulk power system reliability evaluation considering optimal transmission switching and dynamic line thermal rating," in *Probabilistic Methods Applied to Power Systems* (PMAPS), 2016 International Conference on, Beijing, China, 2016.
- [43] R. Billinton and A. Jonnavithula, "Variance reduction techniques for use with sequential Monte Carlo simulation in bulk power system reliability evaluation," in *Proc. Canadian Conf. on Elect. and Comp. Eng.*, vol. 1, Calgary, Canada, May 1996, pp. 416-419.
- [44] S. Dehghan, N. Amjady, and A. Kazemi, "Two-Stage Robust Generation Expansion Planning: A Mixed Integer Linear Programming Model," *IEEE Trans. Power Syst.*, vol. 29, no. 2, pp. 584-597, Mar. 2014.
- [45] B. Chen, J. Wang, L. Wang, Y. He, and Z. Wang, "Robust optimization for transmission expansion planning: minimax cost vs. minimax regret," *IEEE Trans. Power Syst.*, vol. 29, no. 6, pp. 3069-3077, Nov. 2014.
- [46] Reliability Test System Task Force, "The IEEE Reliability Test System-1996," *IEEE Trans. Power Syst.*, vol. 14, no. 3, pp. 1010-1020, Aug. 1999.
- [47] M Pantos, "Market-based congestion management in electric power systems with increased share of natural gas dependent power plants," *Energy*, vol. 36, no. 7, pp. 4244-4255, 2011.
- [48] A. Moreira, A. Street, and J. Arroyo, "An adjustable robust optimization approach for contingency-constrained transmission expansion planning," *IEEE Trans. Power Syst.*, vol. 30, no. 4, pp. 2013-2022, Jul. 2015.
- [49] A. Conejo, M. Carrion, and J. Morales, Decision Making Under Uncertainty in Electricity Markets. New York, NY, USA: Springer, 2010.
- [50] C. Wang, W. Wei, J. Wang, F. Liu, F. Qiu, C. M. Correa-Posada, and S. Mei, "Robust defense strategy for gas-electric systems against malicious attacks", *IEEE Trans. Power Syst.*, to be published.
- [51] http://people.clarkson.edu/~lwu/data/Gas Elec Planning/.
- [52] Electric Reliability Council of Texas (ERCOT), Market Information, 2014, [Online]. Available: http://ercot.com/mktinfo/.
- [53] S. Wogrin, P. Dueñas, A. Delgadillo and J. Reneses, "A new approach to model load levels in electric power systems with high renewable penetration," *IEEE Trans. Power Syst.*, vol. 29, no. 5, pp. 2210-2218, Sept. 2014.
- [54] J. López, K. Ponnambalam, and V. Quintana, "Generation and transmission expansion under risk using stochastic programming," *IEEE Trans. Power Syst.*, vol. 22, no. 3, pp. 1369-1378, Aug. 2007.
- [55] J. Wang, M. Shahidehpour, and Z. Li, "Security-constrained unit commitment with volatile wind power generation," *IEEE Trans. Power* Syst., vol. 23, no. 3, pp. 1319-1327, Aug. 2008.
- [56] New York Independent System Operator, "2015 congestion assessment and resource integration study, CARIS-Phase I," Nov. 2015 [Online]. Available: http://www.nyiso.com/public/webdocs/markets_operations/ services/planning/Planning_Studies/Economic_Planning_Studies_(CAR IS)/CARIS_Final_Reports/2015_CARIS_Report_FINAL.pdf.

BIOGRAPHIES

Chuan He (S'13) received the B.S. degree and M.S. degree in electrical engineering from Sichuan University, Chengdu, China in 2011 and 2014, respectively, where he is currently pursuing the Ph.D. degree.

He is a visiting Ph.D. student at Clarkson University, Potsdam, NY, USA from 2015 to 2017. His research interests include robust optimization on power system operation and planning with renewable energy.

Lei Wu (SM'13) received the B.S. degree in electrical engineering and the M.S. degree in systems engineering from Xi'an Jiaotong University, Xi'an,

China, in 2001 and 2004, respectively, and the Ph.D. degree in electrical engineering from Illinois Institute of Technology (IIT), Chicago, IL, USA, in 2008. From 2008 to 2010, he was a Senior Research Associate with the Robert W. Galvin Center for Electricity Innovation, IIT. He worked as summer Visiting Faculty at NYISO in 2012. Currently, he is an Associate Professor with the Electrical and Computer Engineering Department, Clarkson University, Potsdam, NY, USA. His research interests include power systems operation and planning, energy economics, and community resilience microgrid.

Tianqi Liu (SM'16) received the B.S. and the M.S. degrees from Sichuan University, Chengdu, China, in 1982 and 1986, respectively, and the Ph.D. degree from Chongqing University, Chongqing, China, in 1996, all are in Electrical Engineering. Currently, she is a professor in school of electrical engineering and information at Sichuan University. Her main research interests are power system analysis and stability control, HVDC, optimal operation, dynamic security analysis, dynamic State Estimation and load forecast.

Zhaohong Bie (SM'12) received the B.S. and M.S. degrees from the Department of Electric Power, Shandong University, Jinan, China, in 1992 and 1994, respectively, and the Ph.D. degree from Xi'an Jiaotong University, Xi'an, China, in 1998. She is currently a Professor in the State Key Laboratory of Electrical Insulation and Power Equipment and the School of Electrical Engineering, Xi'an Jiaotong University. Her main research interests include power system planning and reliability evaluation, as well as the integration of the renewable energy.